

## Structural Models of the Bimetallic Subunit at the A-Cluster of Acetyl Coenzyme A Synthase/CO Dehydrogenase: Binuclear Sulfur-Bridged Ni–Cu and Ni–Ni Complexes and Their Reactions with CO

Todd C. Harrop,<sup>†</sup> Marilyn M. Olmstead,<sup>‡</sup> and Pradip K. Mascharak<sup>\*†</sup>

Department of Chemistry and Biochemistry, University of California, Santa Cruz, California 95064, and  
Department of Chemistry, University of California, Davis, California 95616

Received August 4, 2004; E-mail: pradip@chemistry.ucsc.edu

The bacterial metalloenzyme acetyl coenzyme A synthase/CO dehydrogenase (ACS/CODH) catalyzes two very important biological processes, namely the reduction of atmospheric CO<sub>2</sub> to CO and the synthesis of acetyl coenzyme A from CO, CH<sub>3</sub> from a methylated corrinoid iron–sulfur protein, and the thiol coenzyme A.<sup>1</sup> The structure of the A-cluster, where ACS synthesis occurs, has recently been determined by crystallography.<sup>2,3</sup> Two separate A-cluster structures of ACS/CODH from the bacterium *Moorella thermoacetica* reveal a multimetallic active site containing a cuboidal Fe<sub>4</sub>S<sub>4</sub> unit bridged to a bimetallic subunit through one Cys-S moiety. The bimetallic site contains a square-planar Ni(II)<sub>d</sub> site (distal to the cubane) coordinated to two deprotonated carboxamido nitrogens from the peptide backbone and two cysteine sulfurs. The other metal center, designated as the proximal metal (M<sub>p</sub>), contains either a Cu,<sup>2</sup> Ni,<sup>3</sup> or Zn<sup>3</sup> ion and is bridged to the Ni<sub>d</sub> site through two Cys-S residues and to the Fe<sub>4</sub>S<sub>4</sub> unit through one other Cys-S, affording an M<sub>p</sub>(Cys-S)<sub>3</sub> coordination sphere. In addition to the three bridging Cys-S moieties, a fourth, still unidentified, ligand is also bound to complete the coordination sphere. An intense debate over the roles of three different metal ions has recently been subsided following careful biochemical studies<sup>4</sup> and publication of a third A-cluster structure from the hydrogenogenic bacterium *Carboxydotherrmus hydrogenoformans*.<sup>5</sup> It is now evident that Ni occupies the M<sub>p</sub> site in the catalytically active enzyme; both Cu and Zn found in the crystal had their origin in the promiscuity of adventitious metal ion capture by the Ni<sub>d</sub> site.<sup>4</sup>

The quest for insight into the mechanism of acetyl coenzyme A synthesis on the basis of the crystal structures has prompted us<sup>6</sup> and others<sup>7</sup> to synthesize structural analogues of the active site. In these attempts, the Fe<sub>4</sub>S<sub>4</sub> unit has often been ignored (unlikely substrate binding site) and the focus has been primarily on the M<sub>p</sub>–Ni<sub>d</sub> bimetallic site. In this Communication, we report the results of our modeling attempt(s) that utilizes the Ni(II)–dicarboxamido-dithiolato complexes (Et<sub>4</sub>N)<sub>2</sub>[Ni(NpPepS)] (**1**)<sup>6b</sup> and (Et<sub>4</sub>N)<sub>2</sub>[Ni(PhPepS)] (**2**) as Ni<sub>d</sub> synthons in the construction of Ni–Cu and Ni–Ni dinuclear analogues (Figure 1).

Treatment of an MeCN solution of **1** with 1 equiv of [Cu(neo)-Cl] (neo = 2,9-dimethyl-1,10-phenanthroline) afforded the brown dinuclear Ni–Cu complex (Et<sub>4</sub>N)[Cu(neo)Ni(NpPepS)] (**3**) (Figure 2) in 70% yield. Crystallographic analysis of **3** reveals a square planar Ni(II) ion bridged to a distorted tetrahedral Cu(I) center via the thiolato-S donors of **1**. The average Cu–S and Ni–S distances of **3** (2.2934 and 2.1950 Å, respectively) compare well with those observed in the Cu form of ACS/CODH.<sup>2</sup> The Cu–Ni distance of **3** (3.0740 Å) is somewhat longer than that of the enzyme (2.792 Å). Steric constraints imposed by the NpPepS<sup>4-</sup> ligand frame are presumably responsible for the longer metal–metal distance.

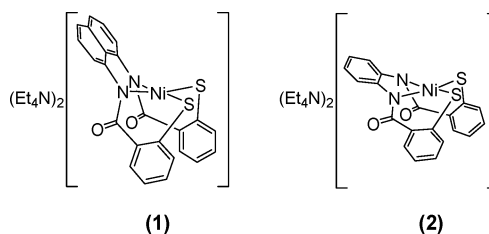


Figure 1. Ni(II) synthons (Ni<sub>d</sub> mimics) used in this study.

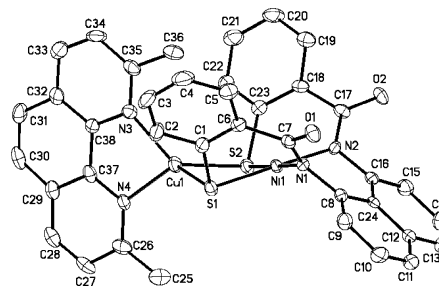


Figure 2. ORTEP diagram of the anion of (Et<sub>4</sub>N)[Cu(neo)Ni(NpPepS)] (**3**) (50% probability) with the atom-labeling scheme. H atoms are omitted for the sake of clarity. Selected bond distances (Å) and bond angles (°): Cu–N(3) 2.037(5), Cu–S(1) 2.2670(16), Ni–N(1) 1.889(5), Ni–S(1) 2.1876(15), Ni–Cu 3.0740(11), N(3)–Cu–N(4) 82.66(18), N(3)–Cu–S(1) 129.79(14), N(4)–Cu–S(2) 115.91, S(1)–Cu–S(2) 87.46(6), N(1)–Ni–N(2) 88.75(19), N(2)–Ni–S(1) 177.80(15), S(1)–Ni–S(2) 92.49(6), C(1)–S(1)–Ni 101.17(18).

Interestingly, the cathodic cyclic voltammogram of **3** in DMF does not exhibit any reduction wave up to –1.8 V (vs SCE). It is therefore evident that the Ni(II) center of **3** (Ni<sub>d</sub> mimic) is very resistant to reduction. The metal centers of **3** show no affinity toward CO,<sup>7c</sup> and passage of CO through solutions of **3** results in no breakdown of the complex. This latter behavior of **3** contrasts that of similar Ni(II)–Cu(I) sulfur-bridged complexes.<sup>7b</sup>

The reaction of [Ni(terpy)Cl<sub>2</sub>] (terpy = 2,2':6',2''-terpyridine) and **1** (1:1 ratio) in MeCN resulted in the isolation of neutral [Ni(terpy)Ni(NpPepS)] (**4**) as a red-brown powder (75%). Since the A-cluster exhibits an EPR spectrum (NiFeC signal) upon one-electron reduction and CO binding (A<sub>red</sub>-CO), we explored the possibility of reduction and CO binding with the Ni–Ni dimer **4**. Upon reduction of **4** to **4**<sub>red</sub> with Na<sub>2</sub>S<sub>2</sub>O<sub>4</sub>, an axial EPR spectrum (100 K, DMF glass) is observed (*g* = 2.226, 2.125). This spectrum is characteristic of five-coordinate Ni(I) in a trigonal bipyramidal geometry.<sup>8</sup> Reaction of CO with **4**<sub>red</sub> in DMF results in **4**<sub>red</sub>-CO adduct with a terminal Ni(I)–CO band at 2044 cm<sup>-1</sup>. In DMF glass, **4**<sub>red</sub>-CO displays a rhombic EPR spectrum with *g* = 2.223, 2.128, 2.019 (Figure S1, Supporting Information), typical of similar six-coordinate Ni(I) compounds with terminally bound CO molecule.<sup>8</sup> Since **4** does not exhibit any affinity toward CO, it is evident that the Ni<sub>p</sub> mimic in this model only binds CO in the reduced (+1)

<sup>†</sup> University of California, Santa Cruz.

<sup>‡</sup> University of California, Davis.

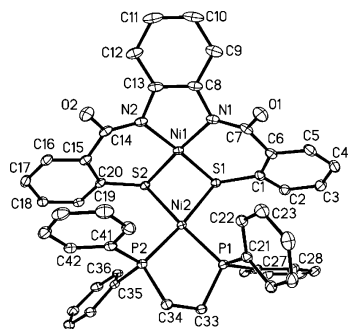


**Figure 3.** ORTEP diagram of  $[\text{Ni}(\text{dppe})\text{Ni}(\text{PhPepS})]$  (**6**) (50% probability) with the atom-labeling scheme. H atoms are omitted for the sake of clarity. Selected bond lengths ( $\text{\AA}$ ) and bond angles ( $^\circ$ ): Ni1–Ni2 2.8255(4), Ni1–N1 1.8909(17), Ni1–N2 1.8895(17), Ni1–S1 2.1558(5), Ni1–S2 2.1438(5), Ni2–S1 2.2354(6), Ni2–S2 2.2413(5), Ni2–P1 2.1781(6), Ni2–P2 2.1816(6), S2–Ni1–S1 79.29(2), P1–Ni2–P2 86.18(2), Ni1–S1–Ni2 80.077(19), C1–S1–Ni 111.15(17).

state. The  $\text{Ni}_d$  mimic **1** shows no affinity toward CO under similar reducing conditions, and no EPR signal is observed.

Since the  $\text{Ni}_p$  site in ACS is four-coordinate in the resting state, we attempted synthesis of appropriate Ni–Ni models with a second  $\text{Ni}_p$  synthon,  $[\text{Ni}(\text{dppe})\text{Cl}_2]$  (dppe = 1,2-bis(diphenylphosphino)ethane). This  $\text{Ni}_p$  synthon is expected to favor an easier reduction to the Ni(I) oxidation state and further facilitate binding of CO. However, due to the geometric constraints imposed by the ligand frame in **1**, all attempts to synthesize the Ni–Ni complex with  $[\text{Ni}(\text{dppe})\text{Cl}_2]$  eventually led to the formation of trimeric  $(\text{Et}_4\text{N})_2[\text{Ni}(\text{DMF})_2\{\text{Ni}(\text{NpPepS})\}_2]$  (**5**, Scheme S1, Supporting Information). We therefore synthesized the second  $\text{Ni}_d$  synthon  $[\text{Ni}(\text{PhPepS})]^{2-}$  (anion of **2**, structure shown in Figure S2, Supporting Information), employing a ligand with less steric demands. Reaction of **2** with 1 equiv of  $[\text{Ni}(\text{dppe})\text{Cl}_2]$  in MeCN afforded  $[\text{Ni}(\text{dppe})\text{Ni}(\text{PhPepS})]$  (**6**, Figure 3) as a blue-green crystalline solid in 85% yield. In this Ni–Ni model, the two Ni(II) centers are bridged through both thiolato-S donors of the PhPepS $^{4-}$  ligand frame, and both exist in square planar geometry. The dihedral angle between the two square planes is  $111.4^\circ$ , and the Ni–Ni separation is 2.8255(4)  $\text{\AA}$ . The metric parameters of the bridged  $\text{Ni}_d$  synthon in **6** are very similar to that noted with **2**. This suggests that sulfur metalation does not change any structural feature of this  $\text{Ni}_d$  mimic. Complex **6** can be easily reduced with  $\text{Na}_2\text{S}_2\text{O}_4$  or  $\text{NaBH}_4$ , and **6**<sub>red</sub> exhibits a strong Ni(I) EPR spectrum similar to other Ni(I)- $\text{P}_2\text{S}_2$  complexes.<sup>9</sup> Since **2** does not exhibit any reduction wave up to  $-1.8$  V vs SCE in solvents such as DMF, it is clear that the reduction occurs at the  $\text{Ni}_p$  site of **6**. Although **6** displays no reactivity toward CO, the one-electron-reduced species **6**<sub>red</sub> is different. Passage of CO through a DMF solution of **6**<sub>red</sub> generates the CO adduct **6**<sub>red</sub>-CO (EPR spectrum shown in Figure S3, Supporting Information) that displays a strong  $\nu_{\text{CO}}$  band at 1997  $\text{cm}^{-1}$ , consistent with a terminal Ni(I)-CO unit.<sup>10</sup> One must note that this  $\nu_{\text{CO}}$  value is very close to the enzyme value of 1996  $\text{cm}^{-1}$ .<sup>11</sup> Rauchfuss and co-workers have reported a dinuclear Ni complex in which two molecules of CO are bound to a Ni(0) center in terminal fashion.<sup>7c</sup> This species displays two  $\nu_{\text{CO}}$  bands at 1948 and 1866  $\text{cm}^{-1}$ . Since these  $\nu_{\text{CO}}$  values are lower than that of the enzyme, it is quite possible that the  $\text{Ni}_p$  site in ACS does not attain the 0 oxidation state during catalysis. Recently, two groups have reported sulfur-bridged dinuclear Ni complexes with  $\text{P}_2\text{S}_2$  coordination at the bridged Ni center that exhibit low reduction potentials.<sup>7a,e</sup> However, no spectroscopic data are available on the CO adducts of these complexes in the reduced state. Complex **6** is therefore the first structurally characterized Ni–Ni model that includes dicarboxamide-dithiolate ligation ( $\text{Ni}_d$  mimic) with a bridged Ni(II) center that

can be reduced to the Ni(I) state and binds CO in terminal fashion ( $\text{Ni}_p$  mimic).

Several groups have shown that the ACS activity and the NiFeC signal of the enzyme diminish upon treatment with 1,10-phenanthroline (phen), whereupon part of the Ni is removed (labile Ni).<sup>1,12</sup> Treatment of **1** or **2** with excess phen (up to 100 equiv) does not lead to the formation of  $[\text{Ni}(\text{phen})_3]^{2+}$ . However, when **6** is treated with excess phen ( $\sim 25$  equiv) in  $\text{CH}_2\text{Cl}_2$ , the electronic absorption spectrum of **6** changes to that of the monomer **2** and  $[\text{Ni}(\text{phen})_3]^{2+}$  over a time period of 35 min, with  $k_{\text{obs}} = 1.502 \times 10^{-4} \text{ s}^{-1}$  (Figure S4, Supporting Information). This reaction confirms that the thiolato-S bridges between the  $\text{Ni}_d$  and the  $\text{Ni}_p$  centers in models such as **6** are vulnerable to phen treatment. Since phen does not remove Ni from the  $\text{Ni}_d$  synthons **1** and **2**, it is apparent that the labile Ni in the enzyme arises from the  $\text{Ni}_p$  site. Interestingly, addition of excess (up to 100 equiv) neocuproine, a Cu(I) chelator, to **6** does not result in any Ni loss. These observations are in line with those observed with the enzyme.<sup>4a,c</sup>

In summary, we report two Ni–Ni models, namely **4** and **6**, that exhibit structural features and chemical properties very similar to those of the binuclear active site of ACS/CODH. These models are the first examples of sulfur-bridged dinuclear Ni complexes that bind CO at the bridged Ni(I) center, as proposed in the mechanism of acetyl coenzyme A synthesis.<sup>3</sup> Also, in one case, the corresponding Ni–Cu model has been characterized.

**Acknowledgment.** T.C.H. received support from the NIH IMSD grant GM58903.

**Supporting Information Available:** Spectroscopic and analytical data for the complexes; Scheme S1 summarizing the synthetic reactions; X-band EPR spectra of **4**<sub>red</sub> and **4**<sub>red</sub>-CO (Figure S1) and **6**<sub>red</sub>-CO (Figure S3); ORTEP diagram of  $(\text{Et}_4\text{N})_2[\text{Ni}(\text{PhPepS})]$  (**2**) (Figure S2); changes in the electronic absorption spectrum of **6** upon phen addition (Figure S4); and X-ray crystallographic files in CIF format. This material is available free of charge via the Internet at <http://pubs.acs.org>.

## References

- Ragsdale, S. W.; Kumar, M. *Chem. Rev.* **1996**, *96*, 2515–2539.
- Doukov, T. I.; Iverson, T. M.; Seravalli, J.; Ragsdale, S. W.; Drennan, C. L. *Science* **2002**, *298*, 567–572.
- Darnault, C.; Volbeda, A.; Kim, E. J.; Legrand, P.; Vernede, X.; Lindahl, P. A.; Fontecilla-Camps, J.-C. *Nat. Struct. Biol.* **2003**, *10*, 271–279.
- (a) Seravalli, J.; Xiao, Y.; Gu, W.; Cramer, S. P.; Antholine, W. E.; Krymov, V.; Gerfen, G. J.; Ragsdale, S. W. *Biochemistry* **2004**, *43*, 3944–3955. (b) Webster, C. E.; Darensbourg, M. Y.; Lindahl, P. A.; Hall, M. B. *J. Am. Chem. Soc.* **2004**, *126*, 3410–3411. (c) Bramlett, M. A.; Tan, X.; Lindahl, P. A. *J. Am. Chem. Soc.* **2003**, *125*, 9316–9317. (d) Schenker, R. P.; Brunold, T. C. *J. Am. Chem. Soc.* **2003**, *125*, 13962–13963.
- Svetlichnyi, V.; Dobbek, H.; Meyer-Klaucke, W.; Meins, T.; Thiele, B.; Römer, P.; Huber, R.; Meyer, O. *Proc. Natl. Acad. Sci. U.S.A.* **2004**, *101*, 446–451.
- (a) Harrop, T. C.; Olmstead, M. M.; Mascharak, P. K. *Chem. Commun.* **2004**, 1744–1745. (b) Harrop, T. C.; Olmstead, M. M.; Mascharak, P. K. *Inorg. Chim. Acta* **2002**, *338*, 189–194.
- (a) Krishnan, R.; Riordan, C. G. *J. Am. Chem. Soc.* **2004**, *126*, 4484–4485. (b) Krishnan, R.; Voo, J. K.; Riordan, C. G.; Zahkarov, L.; Rheingold, A. L. *J. Am. Chem. Soc.* **2003**, *125*, 4422–4423. (c) Linck, R. C.; Spahn, C. W.; Rauchfuss, T. R.; Wilson, S. R. *J. Am. Chem. Soc.* **2003**, *125*, 8700–8701. (d) Golden, M. L.; Rampersad, M. V.; Reibenspies, J. H.; Darensbourg, M. Y. *Chem. Commun.* **2003**, 1824–1825. (e) Wang, Q.; Blake, A. J.; Davies, E. S.; McInnes, E. J. L.; Wilson, C.; Schröder, M. *Chem. Commun.* **2003**, 3012–3013.
- (a) Marganian, C. A.; Vazir, H.; Baidya, N.; Olmstead, M. M.; Mascharak, P. K. *J. Am. Chem. Soc.* **1995**, *117*, 1584–1594. (b) Baidya, N.; Olmstead, M. M.; Whitehead, J. P.; Bagyinka, C.; Maroney, M. J.; Mascharak, P. K. *Inorg. Chem.* **1992**, *31*, 3612–3619.
- (a) Kim, J. S.; Reibenspies, J. H.; Darensbourg, M. Y. *J. Am. Chem. Soc.* **1996**, *118*, 4115–4123. (b) James, T. L.; Smith, D. M.; Holm, R. H. *Inorg. Chem.* **1994**, *33*, 4869–4877. (c) Bowmaker, G. A.; Boyd, P. D. W.; Campbell, G. K.; Hope, J. M.; Martin, R. L. *Inorg. Chem.* **1982**, *21*, 2403–2412.
- Stoppioni, P.; Dapporto, P.; Sacconi, L. *Inorg. Chem.* **1978**, *17*, 718–725.
- Chen, J.; Huang, S.; Seravalli, J.; Gutzman, H., Jr.; Swartz, D. J.; Ragsdale, S. W.; Bagley, K. A. *Biochemistry* **2003**, *42*, 14822–14830.
- Shin, W.; Lindahl, P. A. *Biochemistry* **1992**, *31*, 12870–12875.

JA045284S